Dynamics of periodic pattern formation

H. R. Schober, E. Allroth, K. Schroeder, and H. Müller-Krumbhaar
Institut für Festkörperforschung der Kernforschungsanlage Jülich, D-5170 Jülich, Federal Republic of Germany
(Received 23 July 1985)

The formation of a one-dimensional periodic pattern from an originally homogeneous infinite system is analyzed. We develop a mean-field-like theory for the structure function. The method gives predictions for the temporal evolution towards the final stationary state. It predicts a shift of the finally selected wave vector away from the maximum of the linear spectrum. Numerical simulation confirms this behavior for intermediate times but shows a "lock-in" of the pattern with subsequent conservation of "nodes." Thus the final wave vector in general is neither the one predicted by our modified mean-field calculation nor one of those predicted by other selection criteria based on stationary solutions only. At long times a phase diffusion regime is observed where the node distances equilibrate. This results in a $t^{-1/4}$ law for the width of the structure function which can be understood in terms of a linear diffusion equation for the phase by assuming a random distribution of the gradient of the phase at the lock-in time.

I. INTRODUCTION

Spatially extended continuous dissipative systems often tend to form stationary periodic patterns. Examples are the Rayleigh-Bénard instability of convection, the formation of cellular interfaces in crystal growth, or spatial patterns in chemical reactions like *Liesegang* rings. The underlying mathematical models, nonlinear partial differential equations, typically give a continuous band of solutions in an interval $Q=[\hat{k}^1,\hat{k}^2]$ of the wave number k of the basic periodicity, where a solution within this band is stable against small-amplitude perturbations.

One of the most intriguing questions in this context concerns the ultimately selected wave number k—depending on initial conditions, boundary conditions, and external noise—and the dynamics of evolution towards this pattern. Several different selection principles have been proposed[1-10] to answer the question of which pattern is to be selected. If the equation of motion can be derived from a Lyapunov functional, one has the principle of minimizing this functional.[1,2,5] The second principle,[4,6] containing this first one as a special case, is based on a balance of forces between solutions of different k value and is not restricted to systems derivable from a potential function. The third idea[7] is a phase-space argument. It assumes that the system selects the mode most susceptible to external noise. A quite different approach deals with the formation of periodic patterns via front propagation. It seems to apply to cases where the fluctuations responsible for the instability of the homogeneous system are sharply localized in space. The resulting pattern is governed by the "marginal stability" principle.[9,10] The selected wavelength does not correspond to the ones obtained by the previous arguments.[5,6]

Thus, one is led to the conclusion that a static criterion is not sufficient to determine the finally selected pattern, even when the external boundaries are so far away that the only important length scales are given by the interval Q of the possible wave numbers. Nevertheless, one may hope that the process of pattern selection still has some universal features such that one may define a set of dynamical classes of problems with equivalent behavior.

One obvious criterion concerns the type of fluctuations triggering the instability of the initially homogeneous system. If the fluctuations are spatially localized, pattern selection will be via front propagation.[9,10] If, however, the fluctuations are spatially extended, the system will first develop periodic structures over finite regions in space. The final state is then a result of the competition between these different regions.

In many cases such an instability of a homogeneous system towards pattern formation occurs only when some control parameter exceeds a critical value. An example is the Rayleigh number in Rayleigh-Bénard experiments. An approximate description of the dynamics of this system in the close neighborhood of the critical Rayleigh number is achieved by a complex amplitude equation.[1,2] For small initial perturbations with a broad spectrum in k space it was shown by a multiple-time-scale analysis[2] that the finally selected mode corresponds to the one which minimizes the corresponding Lyapunov functional. Near criticality this also corresponds to the critical value.

For the dynamics of these processes one has at least three different time scales, apart from the short time scale of the triggering fluctuations.[2] Starting from small amplitudes of random perturbations, the instability of the homogeneous system first grows exponentially until the amplitude of the spatially oscillatory pattern is comparable with the final state. Then follows a rearrangement of the "nodes" of the pattern which depends on the nonlinear nature of the problem. The final approach to the stationary periodic state then can be understood as a (linear) diffusion process of the locally varying phase.

Most of the previous analysis of this problem is restricted to the immediate neighborhood of the critical point and to small random amplitudes as initial conditions. In the present investigation we try to gain some insight into the selection process for more general initial conditions

and beyond the critical region. For this purpose we formulate in the following section a mean-field theory for the structure function using a one-dimensional model equation. It resembles the one used in the problem of spinodal decomposition.[11–14] For short times a simple-minded decoupling scheme suffices. For longer times, when the system is approaching a periodic pattern and the structure function is considerably sharpened, a modified mean-field theory is more appropriate. This recovers known results for the critical region but gives predictions for a shift in wave vector outside the critical region towards smaller k values. In Sec. III we present results of extensive numerical studies. They indicate the different time-scales: exponential linear growth of the unstable modes at small times, saturation of the amplitudes and decrease of the width of the structure function, as predicted by the modified mean-field theory, at intermediate times, and, finally, a slow rearrangement of the nodes by phase diffusion after their number has become fixed. The finally selected wave vector turns out to depend on the initial conditions for the structure function in analogy to memory effects found in spin-glass systems.[15] In Sec. IV we analyze the time dependence of the width of the structure function in the phase diffusion regime.

II. MEAN-FIELD DYNAMICS

A simple pattern-forming equation of motion for some one-dimensional field $y(x,t)$ in one space dimension is

$$\frac{\partial}{\partial t}y(x,t)=\mathscr{L}*y(x,t)-y^3(x,t)\ , \tag{1}$$

where $\mathscr{L}$ is a linear operator giving rise to a spatially oscillatory structure. In our calculations we use the Hohenberg-Swift[16] form:

$$\mathscr{L}=\gamma^2-\left[1+\frac{\partial^2}{\partial x^2}\right]^2\ , \tag{2}$$

with $0\le\gamma\le 1$ as the control parameter. The spatial Fourier transform of Eq. (1) is

$$\frac{\partial}{\partial t}y(k,t)=\Omega_k y(k,t) - \int_{-\infty}^{\infty}dq\int_{-\infty}^{\infty}dq'\,y(k-q-q')y(q)y(q') \tag{3}$$

where Ω_k is the Fourier transform of $\mathscr{L}$. It is real with a maximum at $k=1$ and positive for $k^1\le k\le k^2$. Thus, Ω_k causes the homogeneous system to become unstable against perturbations with wave numbers between k^1 and k^2.

The real stationary solutions of Eq. (1) can be given as a Fourier series,[5]

$$y(x,t)=\sum_{l=0}^{\infty}a_{2l+1}\cos[(2l+1)k(x-x_0)]\ . \tag{4}$$

To lowest order in γ the coefficients are $a_{2l+1}\sim\gamma^{2l+1}$, with

$$a_1=(\tfrac{4}{3}\Omega_k)^{1/2}+O(\gamma^2)\ , \qquad a_3=a_1^3/(4\Omega_{3k})+O(\gamma^5)\ . \tag{5}$$

Linear stability analysis has shown that these stationary solutions are stable against small perturbations in a narrower band $k^1\le\hat{k}^1\le k\le\hat{k}^2\le k^2$.

We will now address ourselves to the question which k value out of this band will be selected dynamically starting from a random initial fluctuation. To this end we introduce an equal-time correlation function

$$S(k,t)=\langle y(-k,t)y(k,t)\rangle\ , \tag{6}$$

where the averaging is over initial conditions or equivalently, in the infinite system, over space. From (3) one has

$$\frac{1}{2}\frac{\partial}{\partial t}S(k,t)=\Omega_k S(k,t)-\int_{-\infty}^{\infty}dq\int_{-\infty}^{\infty}dq'\langle y(-k,t)y(k-q-q',t)y(q,t)y(q',t)\rangle\ . \tag{7}$$

The simplest approximation is to decouple the four-point correlation function into three pairs of pair correlation functions (random-phase or mean-field approximation),

$$\frac{1}{2}\frac{\partial}{\partial t}S(k,t)=\left[\Omega_k-3\int_{-\infty}^{\infty}dq\,S(q,t)\right]S(k,t)\ . \tag{8}$$

In this approximation the nonlinearity is independent of k; the different k modes couple only via the total amplitude. This can be utilized to solve the equation exactly:

$$S(k,t)=S(k,0)e^{2\Omega_k t}\left[1+3\int_{-\infty}^{\infty}dq(e^{2\Omega_q t}-1)S(q,0)/\Omega_q\right]^{-1}\ . \tag{9}$$

The relaxation to the final state with $k=1$ proceeds via amplitude relaxation only. This final state is independent of the initial conditions as long as $S(k=1,t=0)\neq 0$. The higher harmonics of the stationary solution (4) are not present and the ground-mode amplitude is reduced by a factor of 2.

This approximation can be shown to give correct results for the early stages of the system evolving from a homogeneous state perturbed by small amplitude fluctuations, but, as in the analogous theory of spinodal decomposition,[8] it breaks down before a true stationary solution (4) of Eq. (1) has been reached. This is due to two major shortcomings of the simple decoupling in Eq. (8). First, it produces an overcounting of terms in the four-point correlation function by a factor 2, when the system becomes coherent over large distances compared to the

characteristic wavelength λ_0. Second, the higher harmonics are assumed to be incoherent with their basic modes.

We are interested in the long-term behavior of the system. In the following, therefore, we describe a decoupling approximation which allows for asymptotically stable solutions. We start from a plausible assumption that the system evolves rather quickly into a state where one can define extended spatial regions (which we number by $l=1,\ldots,n$) with k values k_l close to 1. This is a consequence of the random initial fluctuations which lead to different amplitudes and spectra in different regions of space. The amplitudes in these regions will adjust quickly to the local saturation amplitudes, Eq. (4). We take into account the strong correlation of the pattern within each region but neglect phase coherence between these regions. We formally decompose the system into a sum over regions L_l of finite extents $L_l \gg 2\pi/k_l$ centered at x_l:

$$y(k,t)=\sum_{l=1}^{N} y_l(k,t) \quad \text{with } N\to\infty \ , \tag{10}$$

with a reality condition $y_l(k)=y_l^*(-k)$.

At a sufficiently late stage the regional $y_l(k)$ will have a structure similar to the stationary solution, Eq. (4), i.e., it will consist of nonoverlapping peaks positioned at $(2n+1)k_l$:

$$\begin{aligned} y_l(k,t) &= e^{-ikx_l} \sum_{n=\pm1,\pm3,\ldots} z_l^{(n)}\delta_l^{(n)}(k) l^{i\rho_l^{(n)}} \\ &= e^{-ikx_l} \sum_{n=\pm1,\pm3,\ldots} \psi_l^{(n)}(k) \end{aligned} \tag{11}$$

where $\delta_l^{(n)}$ has an envelope which is peaked at nk_l. Its width is $\sim L_l^{-1}$ and it is normalized by $\int dk\, |\delta_l^{(n)}(k)|^2=1$. $\rho_l^{(n)}$ is the mean phase and $z_l^{(n)}$ the average amplitude of the nth harmonic. The quantities $z_l^{(n)}$, $\rho_l^{(n)}$, $\delta_l^{(n)}$, and $\psi_l^{(n)}$ are all time dependent. As first approximation we assume that the phases $\rho_l^{(n)}$ of adjacent regions are uncorrelated while they are correlated within each region. We define correlation functions $S(k)$ by first averaging over space x', $\langle y(x+x')y(x')\rangle_{x'}$, then Fourier transforming with respect to x, and finally averaging over the random phases $\rho_l^{(n)}$ and using the vanishing overlap between peaks at different nk_l:

$$S(k,t)\cong \frac{1}{N}\sum_{l=1}^{N}\frac{1}{L_l}\sum_{n=\pm1,\pm3,\ldots}(z_l^{(n)})^2\,|\,\delta_l^{(n)}(k)\,|^2 \ . \tag{12}$$

By the same procedure, we obtain, for the nonlinear term of Eq. (1),

$$I_4(k)=\frac{1}{N}\sum_l \frac{1}{L_l}\sum_{\substack{n_1,n_2,\\ n_3,n_4}} \int_{-\infty}^{\infty} dq' \int_{-\infty}^{\infty} dq''\psi_l^{(n_1)}(-k)\psi_l^{(n_2)}(k-q'-q'')\psi_l^{(n_3)}(q')\psi_l^{(n_4)}(q'') \ . \tag{13}$$

$I_4(k)$ has the same peak structure as $S(k)$. We will concentrate on the main peak at $k\simeq k_l\simeq 1$. Noting from the stationary solution, Eqs. (4) and (5), the rapid decay of the amplitudes of the higher harmonics, we can expand Eq. (13). In lowest order only the peaks at $k\simeq\pm1$ will contribute. The next-order contribution contains $z^{(3)}$ linearly and will be considered later. Using the reality condition

$$\psi_l^{(-1)}(-k)=[\psi_l^{(1)}(k)]^* \ ,$$

the lowest-order contribution is

$$I_4^{(1)}(k)=\frac{3}{N}\sum_l \frac{1}{L_l}\int_{-\infty}^{\infty} dq' \int_{-\infty}^{\infty} dq''[\psi_l^{(1)}(k)]^*\psi_l^{(1)}(k+q'-q'')[\psi_l^{(1)}(q')]^*\psi_l^{(1)}(q'') \ . \tag{14}$$

Since for large times $\psi_l^{(1)}(k)$ will be strongly peaked around $k=k_l$, we approximate Eq. (14) by

$$I_4^{(1)}(k)\simeq\frac{3}{N}\sum_l \frac{1}{L_l^2}\,|\,\psi_l^{(1)}(k)\,|^2\int_0^{\infty} dq\,|\,\psi_l^{(1)}(q)\,|^2 \ . \tag{15}$$

This expression becomes exact for the stationary state where only one k survives. If, instead, we would have a broad but random distribution of k values, we would get, as in the standard mean-field theory, a prefactor 6 instead of 3. In general, one expects a time-dependent prefactor.

As a last approximation we replace the integral in (15) by its l average:

$$\frac{1}{L_l}\int_0^{\infty} dq\,|\,\psi_l^{(1)}(q)\,|^2\simeq\frac{1}{N}\sum_l\frac{1}{L_l}\int_0^{\infty} dq\,|\,\psi_l^{(1)}(q)\,|^2 \ . \tag{16}$$

The idea of this mean-field-like relation is that the scatter in k_l values between different regions is small compared to the inverse correlation length $2\pi/L_l$. In other words, the system is assumed to consist of large regions of wave number k separated by defects at a typical distance $L\simeq 2\pi/\Delta$.

The equation of motion for $\hat{S}(k)$, the main peak contribution at $k\simeq 1$ to the pair correlation function, is obtained by inserting (12), (14), and (16) into (7):

$$\frac{1}{2}\frac{\partial}{\partial t}\hat{S}(k,t)=\Omega_k\hat{S}(k,t)-3\hat{S}(k,t)\int_0^{\infty} dq\,\hat{S}(q,t)-R(k,t) \ . \tag{17}$$

$R(k,t)$ contains the contributions to the main peak from the higher harmonics. As one can see from Eq. (13), to lowest order this contribution is linear in $\psi_l^{(3)}$:

$$R(k,t)=\frac{3}{N}\sum_l \frac{1}{L_l}\int_0^\infty dq'\int_0^\infty dq''\,\psi_l^{(-1)}(-k)\psi_l^{(3)}(k+q'+q'')\psi_l^{(-1)}(-q')\psi_l^{(-1)}(-q'') . \tag{18}$$

From (1) with (11) we can derive an equation of motion for $\psi_l^{(3)}(3k)$:

$$\frac{\partial}{\partial t}\psi_l^{(3)}(3k,t)=\Omega_{3k}\psi_l^{(3)}(3k,t)-\int_0^\infty dq'\int_0^\infty dq''\psi_l^{(1)}(3k-q'-q'')\psi_l^{(1)}(q')\psi_l^{(1)}(q'') . \tag{19}$$

Due to the large decay constant $|\Omega_{3k}|$ ($\Omega_{3k}\simeq -64$ for $k\simeq k_l\simeq 1$), $\psi_l^{(3)}$ will adjust nearly adiabatically to $\psi_l^{(1)}$:

$$\psi_l^{(3)}(3k)\cong\frac{1}{\Omega_{3k}}\int_0^\infty dq'\int_0^\infty dq''\psi_l^{(1)}(3k-q'-q'')\psi_l^{(1)}(q')\psi_l^{(1)}(q'') . \tag{20}$$

Inserting this into Eq. (17) and using a decoupling scheme analogous to the one leading to Eq. (17) yields

$$R(k,t)=(3/\Omega_{3k})\left[\int_0^\infty dq\,\hat{S}(q,t)\right]^2\hat{S}(k,t) . \tag{21}$$

The final (approximate) equation of motion for the main peak is (17) in conjunction with (21). The first two terms on the right-hand side of (17) closely resemble the straightforward mean-field approach to spinodal decomposition,[11–13] which, however, would give a factor 6 in front of the integral. As mentioned above, this is a good description of the short-time behavior. The difference arises because of the here assumed strong correlations within large regions. More elaborate versions give a gliding prefactor in spinodal decomposition,[13,14] which could, in principle, also be incorporated here. The essential difference to the theory of spinodal decomposition is that for our equation the asymptotic pattern settles to a value $k\neq 0$ not *a priori* defined and incorporates the influence of higher harmonics in $R(k,t)$.

Since we have ignored the detailed mechanism of node annihilation and generation between two neighboring regions, we would expect this equation to overestimate the rate of convergence to a final state. To see what the predictions of (17) and (21) are, we assume $\hat{S}(k,t)$ to be strongly peaked around $k_0(t)$, with a peak width (second moment) $w(t)$, and expand $\hat{S}(k,t)$ around this peak. This gives three coupled differential equations:

$$\frac{\partial}{\partial t}\hat{S}(k_0)=A_{k_0}\hat{S}(k_0) , \tag{22a}$$

$$\frac{\partial}{\partial t}k_0=\left[\frac{\partial}{\partial k_0}A_{k_0}\right]w^2 , \tag{22b}$$

$$\frac{\partial}{\partial t}w=\frac{1}{2}\left[\frac{\partial^2}{\partial k_0^2}A_{k_0}\right]w^3 , \tag{22c}$$

$$A_{k_0}=2\Omega_{k_0}-6\int_0^\infty dq\,\hat{S}(q,t)-(6/\Omega_{3k_0})\left[\int_0^\infty dq\,\hat{S}(q,t)\right]^2 . \tag{22d}$$

Explicit trajectories are obtained by inserting, e.g., a Gaussian for for $\hat{S}(k,t)$.

A more convenient variable than $\hat{S}(k_0)$ is the averaged square amplitude $\langle(z^{(1)})^2\rangle$ or the integral over $\hat{S}(k,t)$, which goes to a finite value for $t\to\infty$. In Fig. 1 we give a schematic plot of some typical flow lines for the long-time behavior of $\langle(z^{(1)})^2\rangle$ versus k_0. Parameters of the curves are different initial conditions. The averaged square amplitude $\langle(z^{(1)})^2\rangle$ relaxes exponentially fast to a value where $A_{k_0}\simeq 0$. The width w of the peak decays with a power law,

$$w\sim t^{-1/2} , \tag{23}$$

while the dominant wave vector $k_0(t)$ shifts to its final value k_∞ like

$$k_0(t)-k_\infty\sim t^{-1}\ln t . \tag{24}$$

The shift of this asymptotic value k_∞ away from 1,

$$k_\infty\cong 1-\tfrac{3}{1024}\gamma^4 , \tag{25}$$

including contributions up to the third harmonic $3k_0$, differs by 3 from the shift obtained by minimizing the Lyapunov functional[5] corresponding to Eq. (1). This is possibly due to the simple decoupling leading to Eq. (21), but there is no *a priori* reason that a mode differing from the static minimum could not be preferred dynamically.

The method described here is not restricted to systems with a Lyapunov functional as in (1) and (2), provided the spectrum Ω_k in (3) in real. The main deficiency of our approach is, however, that we completely ignore phase correlations between neighboring subsystems. Nevertheless, close enough to the critical point ($\gamma^2\ll 1$) the contri-

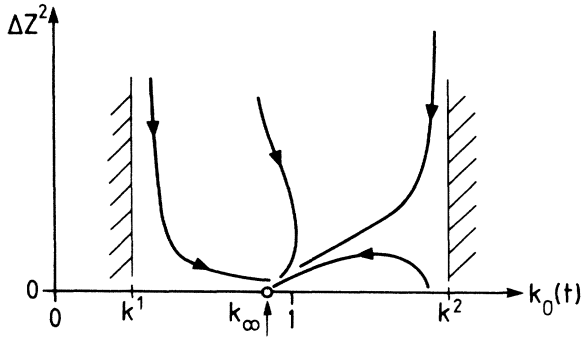

FIG. 1. Temporal development of the averaged amplitude $\Delta z^2=\langle[z^{(1)}(\infty)]^2-[z^{(1)}(t)]^2\rangle$ versus the mean wave vector $k_0(t)$ as predicted by Eq. (22) (schematically). k_∞ is the finally selected wave vector.

bution from the third harmonic becomes irrelevant, and the result of (22) agrees with the exact results for this limit both concerning the selected wave number $k_\infty = 1$ and the diffusional behavior of $w \sim t^{-1/2}$.

III. NUMERICAL ANALYSIS

We have performed a large sequence of numerical integrations of Eqs. (1) and (3) with (2) in real and k space. While the k-space integrations are more efficient for the long-time behavior, the real-space calculations were done as a countercheck on numerical accuracy.

The real-space integrations used a grid of some 25 000 points with a grid spacing $\Delta x \simeq 0.05 \times 2\pi$. This amounts to >1200 full periods of the finally selected structure. For most calculations we used reflective boundary conditions. To check the dependence of the time evolution on the boundary conditions, we also did calculations with diffusive boundary conditions on one end, i.e., we gradually replaced the actual linear operator $\mathscr{L}$, Eq. (2), by $\partial^2/\partial x^2$ at one boundary over the range $\simeq 100$ wavelengths. Derivatives were taken with three- and five- or five- and seven-point formulas for the second and fourth derivatives, respectively. An implicit integration method was used and counterchecked with a four-point Runge-Kutta method.

The k-space integrations used a set of up to 8000 equally spaced modes with spacing $\Delta k < 0.001$. Integration schemes were the same as in real space. A comparison between the two different approaches gave a scatter $< 10^{-3}$ in the number of nodes ultimately obtained which corresponds just about to the discretization error. The dynamical evolution of the structure function also was identical for the two different approaches within the range of the numerical accuracy. We are therefore confident that the numerical results are excellent approximations to the true dynamical behavior of the system.

The initial conditions were typically given by

$$y(k,\, t=0) = \pm A\,(R_k + \tfrac{1}{2})\, e^{-4(k-\bar{k})^2}\,, \tag{26}$$

where the $\pm$ sign was taken at random, $0 \le R_k < 1$ at random, $2\times 10^{-6} \le A \le 2\times 10^{-7}$, $0.8 \le \bar{k} \le 1.2$, and the width of the Gaussian was larger than the width of the interval $[k^1, k^2]$, where $\Omega_k > 0$. For each parameter set $\{A, \bar{k}\}$ ten runs with different independent R_k values were done. The integrations were run over a time such that a single mode was remaining. In time units of Eqs. (1) and (2) this corresponds to times of up to $\approx 10^6$, which are the typical diffusion times of our system.

Figure 2 shows an example for the development of a periodic structure of $y(x,t)$, according to Eq. (1), starting from a random initial state. Already after short times $t \simeq 30$, a quasiperiodic state is reached. More detailed information can be gained from a k-space representation, Figs. 3 and 4. In Fig. 3 we show the time-dependent structure function $\hat{S}(k,t)$ for $\gamma = 0.5$ in the interval $0.6 \le k \le 1.4$ at times $t = 0, 20, 75$. The k spectrum initially was centered at $\bar{k} = 1$. At $t = 20$, $\hat{S}(k,t)$ still looks like a Gaussian, but is considerably sharpened. The random fluctuations seem to have slightly decreased. At $t = 75$, however, the fluctuations around the Gaussian backbone have amplitudes comparable to that backbone. The same happens in Fig. 4, where we have started with a structure centered at $\bar{k} = 0.8$. This indicates the buildup of correlations between different k modes. (Both Figs. 3 and 4 correspond to single runs.)

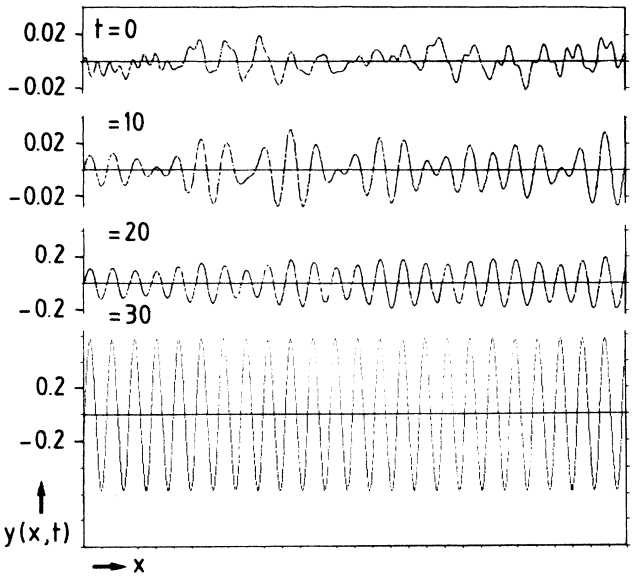

FIG. 2. Numerical example for the evolution of a periodic pattern from a random initial state, according to Eq. (1), $\gamma = 0.5$. Only a short section is shown.

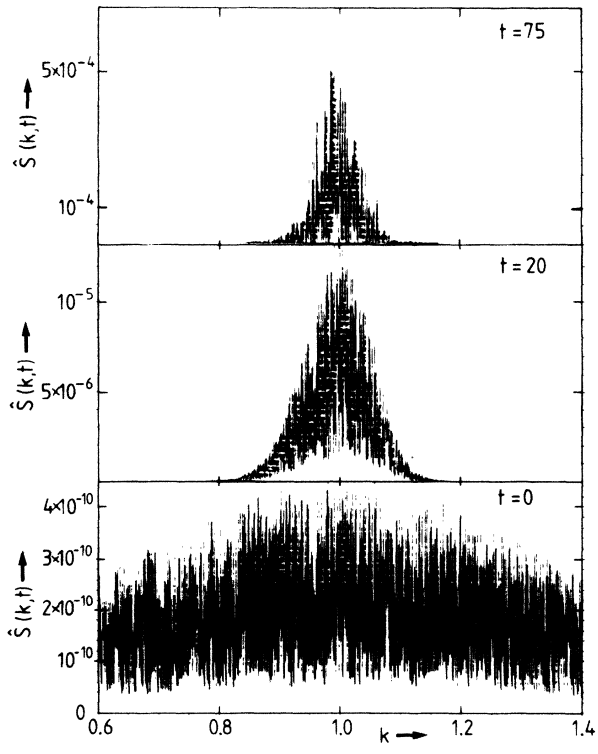

FIG. 3. Evolution of the time-dependent structure function $\hat{S}(k,t)$ for $\gamma = 0.5$ and for $\bar{k} = 1$ starting from small amplitudes (note the different scales).

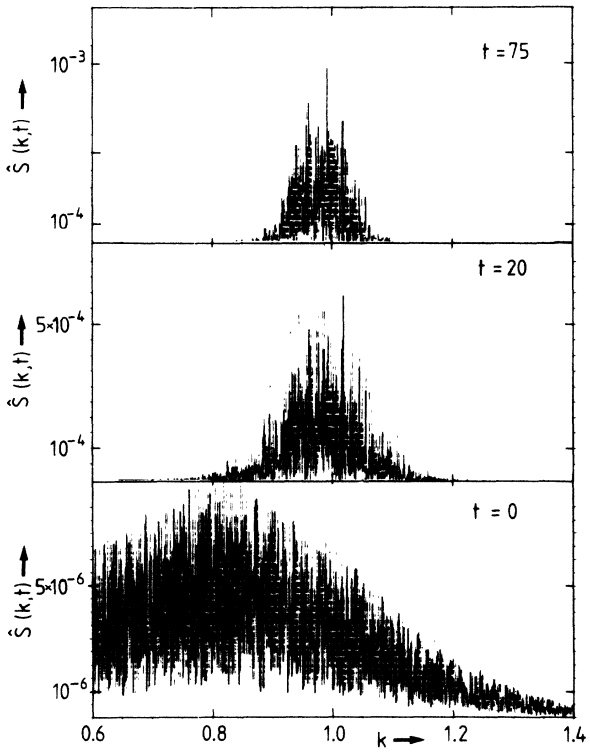

FIG. 4. Evolution of the time-dependent structure function $S(k,t)$ for $\gamma=0.5$ and for $\bar{k}=0.8$ starting from small amplitudes (note the different scales).

To gain more insight we study the time dependence of the lowest momenta of the structure function $\hat{S}(k,t)$, i.e., the amplitude

$$\langle (z^{(1)})^2 \rangle = \int dk\, \hat{S}(k,t) ,$$

the peak position k_0, and the peak width w. For the latter we used the definition

$$w_k = \left[\frac{\int_0^\infty dk\, k^2 \hat{S}(k,t)}{\int_0^\infty dk\, \hat{S}(k,t)} - \left[\frac{\int_0^\infty dk\, k \hat{S}(k,t)}{\int_0^\infty dk\, \hat{S}(k,t)} \right]^2 \right]^{1/2} . \tag{27}$$

To compare with real-space calculations, we introduced a corresponding width w:

$$w_x = \left[\frac{1}{L} \int_0^L dx\, k^2(x) - \left[\frac{1}{L} \int dx\, k(x) \right]^2 \right]^{1/2} , \tag{28}$$

where $k(x)=\pi/\lambda(x)$, and $\lambda(x)$ is the distance between two nodes of $y(x)$. Asymptotically, for nearly periodic structures, the two definitions coincide, as was also found in our simulation.

In Fig. 5 we show for a single run, corresponding to Fig. 3, the time dependence of the square amplitude $\langle (z^{(1)})^2 \rangle$ and the peak width $w(t)$ of the structure function. Starting from small fluctuations $A=2\times10^{-4}$ [Eq. (23)], the amplitude first increases exponentially with time and then practically reaches it final value near times $t\approx10^2$. The width w of the structure function shows a

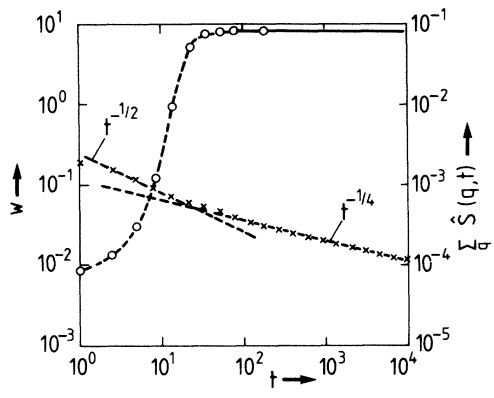

FIG. 5. Peak width w and amplitude $\sum_q \hat{S}(q)$ of the structure function versus time ($\gamma=0.5$). Note the saturation of the amplitude and the change of the power law for $w(t)$ from $t^{-1/2}$ to $t^{-1/4}$ at $t\simeq75$.

behavior consistent with the predicted $t^{-1/2}$ law [Eq. (23)] for the modified mean-field approximation over the intermediate time scale $t\simeq5$ to 50, but then decays considerably slower. For these later times a good fit is given by a $t^{-1/4}$ power law. This continues until times 10^5–10^6 (see also Fig. 7), when, for our system size, the structure function contains only a small number of modes, and therefore it is no longer representative for an infinite system. The width then decays exponentially (not shown), finally leaving a single mode plus its higher harmonics. The calculations show that at the same time, $t\simeq100$, where the amplitude saturates and the time behavior of the width changes from $t^{-1/2}$ to $t^{-1/4}$, also the number of nodes becomes fixed. Therefore, the final k value is already defined and the subsequent dynamics on longer-time scales deals only with the rearrangement of nodes until they become evenly distributed over the full space. We will discuss this phase diffusion in more detail in the subsequent section.

It was already argued previously[2] that the initial state of the system may influence the final selection process. To see this we have varied the initial amplitude A of the fluctuations over 5 orders of magnitude with the spectral distribution centered at $\bar{k}=0.8$, 1.0, and 1.2. Results for the k selection are shown in Fig. 6, where each point represents an average over ten runs with independent initial conditions [R_k of Eq. (23)]. The variance in the final k value was of the order $\simeq5\times10^{-3}$. For very small amplitudes the system finally settles to the value $k=1$ of the most unstable mode, as expected. For large initial amplitudes—corresponding to a turbulent state—the system also tries to settle near $k=1$, but becomes locked at smaller or larger values, dependent on where the initial spectrum was centered. Note that even for $\bar{k}=1$ we obtain a shift to smaller k values. This is still within 1% of $k=1$, but definitely resolvable by our numerical grid of $\Delta k\simeq10^{-3}$. We attribute this latter shift to the fact that Ω_k is not symmetric around its maximum at $k=1$, but dampens the larger k values more strongly than the smaller ones.

These observed shifts are much larger than the ones

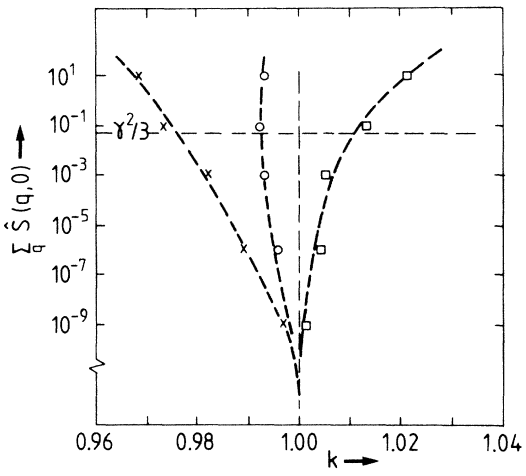

FIG. 6. Final k value k_∞ as a function of the initial amplitude and position of the peak ($\gamma=0.5$). Different symbols indicate different values of the initial position of $\hat{S}(k)$: $\times$, $\bar{k}=0.8$; $\circ$, $\bar{k}=1.0$; $\square$, $\bar{k}=1.2$. The lines connect the results for different initial amplitudes with the same $\bar{k}$. To set the scale for the amplitudes, the dashed line indicates the amplitude of the stationary state at $k=1$, i.e., $\gamma^2/3$.

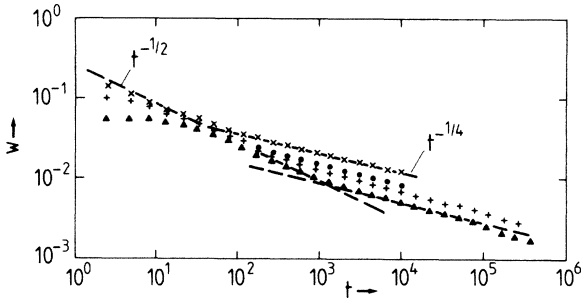

FIG. 7. Decrease of the peak width w with time for various values of γ (average over ten runs each). $\times$, $\gamma=0.5$; $\bullet$, $\gamma=0.3$; $+$, $\gamma=0.2$; $\blacktriangle$, $\gamma=0.1$. The lines indicate the $t^{-1/2}$ and $t^{-1/4}$ decay.

caused by the higher harmonics, as predicted by Eq. (22b): $k_\infty \simeq 1-3\times\gamma^4/1024$. In fact, such small shifts cannot be seen in the simulation. Calculations with a slightly distorted Ω_k, where the amplitude of the higher harmonics is larger, show a shift by these harmonics. This additional shift, however, is less than predicted by Eq. (22b). This can be understood if one considers that the driving term for this shift is proportional to the fourth power of the amplitude. When this saturates at $t\simeq 100$, typically, the number of nodes is fixed, and thus the higher harmonics can induce no further shift.

To check the influence of γ on our findings we varied γ between 0.1 and 0.9. The results are similar. For smaller γ values the final shifts of k_∞ become smaller and vice versa. In Fig. 7 we plot the width of the time-dependent structure function (17) versus the decimal log of the time for different values of the control parameter γ. Initial conditions were as in Fig. 2, with $\bar{k}=1$ and $A=2\times 10^{-6}$. Each curve was averaged over ten independent runs. We have also performed several runs with different initial conditions (varying $\bar{k}$ and A) and obtained the same qualitative behavior. The common feature of all these runs is a discrimination of an intermediate- and a long-time scale. The intermediate-time scale fits the $t^{-1/2}$ law predicted by our modified mean-field approximation, while the longer-time scale gives a behavior like $w\sim t^{-1/4}$. The changeover between these scales varies roughly like $t_c\sim\gamma^{-2}$, as is suggestive from trivial scaling of Eqs. (1)—(3).

IV. PHASE DIFFUSION

In previous papers the final approach to a homogeneous periodic structure was analyzed in terms of phase diffusion.[1,2] In these approaches $y(,x,t)$ is represented as a slowly modulated periodic function:

$$y(x,t)\cong a(\phi(x,t))\cos[k_0 x+\phi(x,t)]+\cdots , \tag{29}$$

where the ellipsis represents unspecified higher-harmonic terms. The amplitude factor $a(\phi(x,t))$ can be shown to adjust very quickly to the local k vector, i.e., to lowest order it is given by

$$a(\phi(x,t))=a_0(t)+a_1(t)[\nabla\phi(x,t)]^2+\cdots . \tag{30}$$

Here, for simplicity, we set $k_0=1$, i.e., to the maximum of the spectrum of the linear operator [Eq. (2)]. In general, the amplitude function would contain an additional term proportional to $\nabla\phi(x,t)$. The final results do not depend on the choice of k_0.

Inserting (29) and (30) into Eq. (1) and expanding with respect to the derivatives of $\phi(x,t)$, we obtain, to lowest order,

$$\{\dot{a}_0+\dot{a}_1(\nabla\phi)^2-\gamma^2[a_0+a_1(\nabla\phi)^2]-4a_0(\nabla\phi)^2-\tfrac{3}{4}a_0^3-\tfrac{9}{4}a_0^2a_1(\nabla\phi)^2\}\cos(x+\phi)+(a_0\dot{\phi}-4a_0\Delta\phi)\sin(x+\phi)=0 . \tag{31}$$

We use the approximate orthogonality of the trigonometric functions for a slowly varying phase $\phi(x,t)$ over a period

$$n\,2\pi\le x+\phi(x,t)\le(n+1)2\pi$$

to separate the time dependence of the amplitudes from the one of the phase. We neglect terms of higher order than $(\nabla\phi)^2$ and $\Delta\phi$, respectively. Finally, we separate the spatially constant and varying amplitude factors. The resulting equations

$$\begin{aligned}\dot{a}_0&=(\gamma^2-\tfrac{3}{4}a_0^2)a_0 ,\\ \dot{a}_1&=(\gamma^2-\tfrac{9}{4}a_0^2)a_1-4a_0 ,\\ \dot{\phi}&=4\,\Delta\phi\end{aligned} \tag{32}$$

show an exponential relaxation of the amplitude factors to their respective asymptotic values:

$$a_0^\infty = 2\gamma/\sqrt{3}, \quad a_1^\infty = -4/(\sqrt{3}\gamma) . \tag{33}$$

The total amplitude $a_0^\infty + a_1^\infty (\nabla\phi)^2$ is the amplitude of a stationary periodic solution with wavelength $k = 1 + \nabla\phi$ to second order in $\nabla\phi$.

The diffusion equation for the phase ϕ yields a power-law behavior for the width of the distribution function. To show that we define the local k vector as

$$k(x) = k_0 + \nabla\phi(x) = 1 + \kappa(x) . \tag{34}$$

The variance of k is calculated according to Eq. (28), which yields

$$w_x^2(t) = \frac{1}{L} \int_0^L dx\, \kappa^2(x,t) , \tag{35}$$

where we have used node conservation as observed in the numerical results:

$$\frac{1}{L} \int_0^L dx\, \nabla\phi(x) = \phi(L) - \phi(0) = 0 . \tag{36}$$

With $\phi(x,t)$, also $\kappa(x,t)$ obeys a diffusion equation which can be solved by Fourier analysis:

$$\kappa(x,t) = \int_0^\infty dq\, e^{-4q^2 t} \tilde{\kappa}(q,0) \cos(qx) , \tag{37}$$

and

$$w_x^2(t) = \frac{\pi}{2L} \int_0^\infty dq\, e^{-8q^2 t} [\kappa(q,0)]^2 . \tag{38}$$

For a further evaluation we have to make an assumption about the distribution of κ values at the onset of the phase diffusion regime. Figure 8 shows numerical results for $|\kappa(q,t)|$ at $t = 75$. They suggest that the $|\kappa|$ distribution oscillates around a constant in the range of the relevant small q values. For sufficiently large systems these oscillations are rapid compared to the variation of the Gaussian in Eq. (38). Thus, the integral is determined by their average and we can approximate Eq. (38) by

$$w_x^2(t) \cong (\pi/2)^{3/2} 1/(4L) \langle [\kappa(q,0)]^2 \rangle_{\text{av}} t^{-1/2} , \tag{39}$$

which yields the numerically observed $t^{-1/4}$ law for the width w of the k distribution.

Physically, the flat distribution means that we have a random fluctuation of the wavelength around the k_∞ value, i.e., small random fluctuations of the gradient of the phase. The sign of $\kappa(q)$ is randomly distributed, which means that the fluctuations in $k(x)$ are homogeneous in space and not localized. For the phase ϕ the flat distribution in $\kappa(q)$ yields $|\phi(q)| \sim 1/q$, which means steplike variations of the phase in real space. Such fluctuations of the wave vector and the phase are consistent with our picture of the system at intermediate times postulated in Sec. II, namely that coherent subsystems evolve with random-phase differences between neighboring regions.

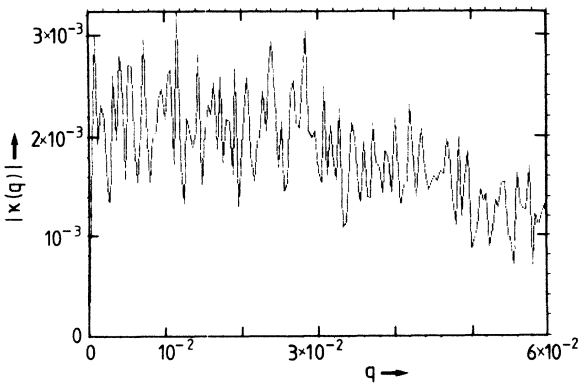

FIG. 8. Example of $|\kappa(q)|$ at the onset of phase diffusion ($\gamma = 0.5$, $t = 75$) averaged over 12 runs. The oscillation amplitude for a single run is much larger.

Our results are in contrast to those of Newell *et al.*[2] for the asymptotic decay of the imaginary part of the complex amplitude equation. The reason seems to be that they implicitly assume a flat distribution for $|\phi(q)|$ for small q, which leads to a $t^{-1/2}$ law for the second cumulant of the phase and, in turn, to a $t^{-3/4}$ behavior for the width of the structure function.

Finally, one could expect nonlinear corrections to the phase diffusion process, since the absolute value of the phase difference between two distant points is not bounded from above. While it seems likely that this would also lead to a slow power law or even logarithmic behavior at intermediate times, the numerical results do not show the necessity for such corrections.

V. CONCLUSIONS

For a simple one-dimensional model equation [Eq. (1)] we have calculated the approach to a stationary periodic pattern starting from a homogeneous initial state with random fluctuations. We have found by numerical and analytical methods that several different time scales can be distinguished in the development of the structure function $S(k,t)$.

At very early times an exponential growth of the initially small amplitudes of the fluctuations is found which can adequately be described by an ordinary mean-field approach. At later times the nonlinear term in Eq. (1) leads to a saturation of the amplitudes. In this regime the mean-field approach has to be modified to account for the strongly peaked structure of $S(k)$. This modification amounts to a change of the prefactor in the mean-field approximation of the nonlinear term, which then leads to the correct amplitudes for the stationary solutions. The nonlinearity also induces growth of the higher harmonics of the instable ground modes, which, in turn, modify the growth of the ground-mode amplitudes. As has been noted earlier,[5] this coupling is one mechanism by which the finally selected wave vector is shifted down from the maximum of the linear spectrum at $k = 1$. However, our numerical calculations show a much more pronounced deviation of the finally selected wave vector. As is clearly demonstrated in Fig. 6, the selected mode is influenced by the initial conditions, i.e., by memory effects similar to features found in spin-glass problems.[15,17] We find that "node conservation" is the mechanism by which this memory is established. When the amplitudes saturate and the structure function sharpens, the system locally locks into a periodic pattern with a wave vector close but not

equal to unity.

The final dynamics concerns the equilibration of the local wave vectors by adjusting the node positions. This is achieved by phase diffusion. Apparently node creation is such a strong perturbation of the system that it is not feasible. At the time when node conservation is established, the time dependence of the width of the structure function changes from the $t^{-1/2}$ behavior predicted by the modified mean-field approximation to a $t^{-1/4}$ behavior (see Fig. 7). This slow convergence can be explained by asymptotically linear phase diffusion assuming a random distribution of the gradient of the position-dependent phase at the time when the final number of nodes has become settled [see Eq. (39)].

[1]A. C. Newell and J. C. Whitehead, J. Fluid Mech. **38**, 279 (1969).

[2]A. C. Newell, C. G. Lange, and P. J. Aucoin, J. Fluid Mech. **40**, 513 (1970).

[3]P. Ortoleva and J. Ross, J. Chem. Phys. **60**, 5090 (1974).

[4]H. Riecke and L. Kramer, Z. Phys. B **59**, 245 (1985).

[5]Y. Pomeau and P. Manneville, J. Phys. (Paris) Lett. **40**, L60 (1979).

[6]L. Kramer, E. Ben-Jacob, H. Brand, and M. C. Cross, Phys. Rev. Lett. **49**, 1891 (1982).

[7]M. Kerszberg, Phys. Rev. A **28**, 1198 (1983).

[8]D. G. Aronson and H. F. Weinberger, *Partial Differential Equations and Related Topics,* Vol. 446 of *Lectures Notes in Mathematics* (Springer, New York, 1975), p. 5.

[9]J. S. Langer and H. Müller-Krumbhaar, Phys. Rev. A **27**, 499 (1983).

[10]G. Dee and J. S. Langer, Phys. Rev. Lett. **50**, 383 (1983).

[11]J. W. Cahn, Trans. Metall. Soc. AIME **242**, 166 (1968).

[12]J. S. Langer, M. Bar-on, and H. D. Miller, Phys. Rev. A **11**, 1417 (1975).

[13]K. Binder, C. Billotet, and P. Mirold, Z. Phys. B **30**, 183 (1978).

[14]H. Horner and K. H. Jüngling, Z. Phys. B **36**, 97 (1979).

[15]W. Kinzel, Phys. Rev. B **19**, 4595 (1979).

[16]J. Swift and P. C. Hohenberg, Phys. Rev. A **15**, 319 (1977).

[17]K. Binder and K. Schröder, Phys. Rev. B **14**, 2142 (1976).

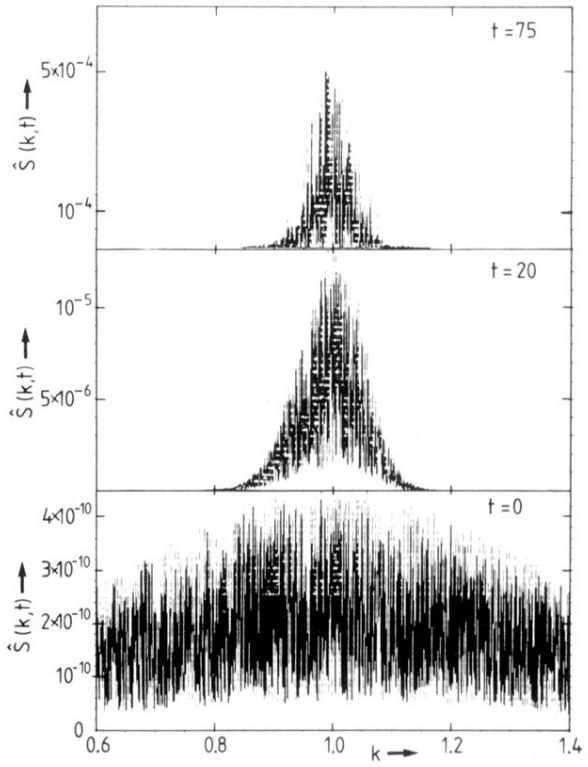

FIG. 3. Evolution of the time-dependent structure function $\hat{S}(k,t)$ for $\gamma=0.5$ and for $\bar{k}=1$ starting from small amplitudes (note the different scales).

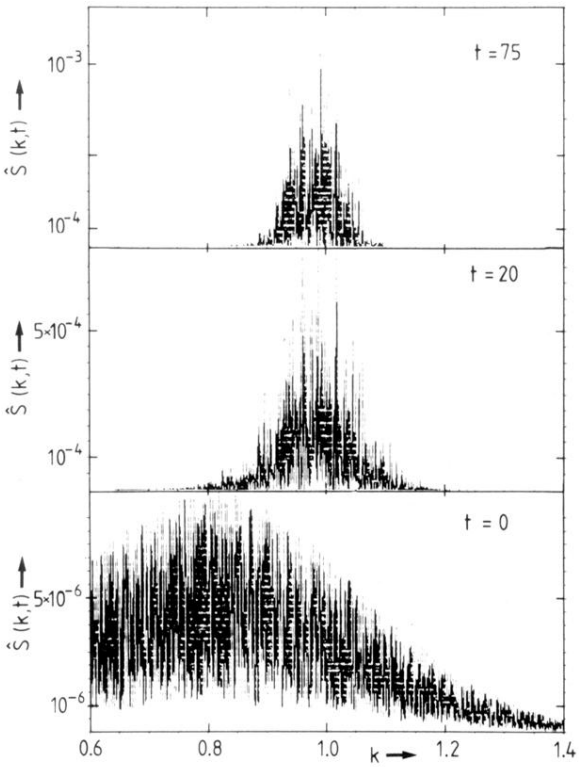

FIG. 4. Evolution of the time-dependent structure function $S(k,t)$ for $\gamma=0.5$ and for $\overline{k}=0.8$ starting from small amplitudes (note the different scales).